

Analysis and shape optimization of variable thickness box girder bridges in curved platform

[M. Özakça](#) and [N. Tavşi](#)

Department of Civil Engineering, University of Gaziantep, Gaziantep, Turkey.

Email: ozakca@gantep.edu.tr, taysi@gantep.edu.tr

ABSTRACT

This paper deals with the development of reliable and efficient computational tools to analyze and find optimum shapes of box girder bridges in curved platform in which the strain energy or the weight of the structure is minimized subject to certain constraints. The finite strip method is used to determine the stresses and displacements based on Mindlin-Reissner shell theory. An automated analysis and optimization procedure is adopted which integrates finite strip analysis, parametric cubic spline geometry definition, automatic mesh generation, sensitivity analysis and mathematical programming methods. It is concluded that the finite strip method offers an accurate and inexpensive tool for the optimization of box girder bridges having regular prismatic-type geometry with diaphragm ends and in curved platform.

KEY WORDS: Box girder bridges, shape optimization, finite strip analysis, Mindlin-Reissner shell theory, strain energy.

1 Introduction

In structural design it is necessary to obtain an appropriate geometric shape for the structure so that it can carry the imposed loads safely and economically. This may be achieved by the use of Structural Shape Optimization (SSO) procedures in which the shape or the thickness of the components of the structure is varied to achieve a specific objective satisfying certain constraints. Such procedures are iterative and involve several re-analyses before an optimum solution can be achieved. SSO tools can be developed by the efficient integration of structural shape definition procedures, automatic mesh generation, structural analysis, sensitivity analysis and mathematical programming methods.

1.1 Literature survey

Single or multi cell box cross sections often appear in single or multispan medium- and long-span bridges. Maisel [1] conducted a detailed survey of the box girder bridges built worldwide until 1970. The usual types of bridges were not economical for long spans because of the rapid increase in the ratio of dead load to total design load as the span lengths increased. The box girder concrete bridge was developed as a solution to this problem.

In practice several methods with various degrees of rigor are available for analysis. These range from the elementary or engineer's beam theory to complex-shell finite element analyses; other methods of analysis utilize folded-plate [2] and [3] methods. Razaqpur and Li [4] developed a straight multicell box girder finite element with exact shape functions based on this extended version of Vlasov's thin walled beam and then they combine Vlasov's thin walled beam theory with the finite element technique to analyze curved multicell box girder bridges [5]. Dawe and Peshkam [6] have presented finite strips formulations for the buckling and vibration of finite length composite prismatic plate structures with diaphragm ends.

The finite strip method, which is now routinely used to gain insight into the structural behavior of prismatic structures, was initially developed by Cheung [3] who presented a wide range of solutions for the static and dynamic analysis of prismatic plates and shells using Kirchhoff's

classical thin plate theory Since its initial introduction by Cheung [3], many authors have investigated the applicability of the finite strips method and have developed many useful extensions. One area of research has been concerned with the development of finite strips models for plates and shells based on Mindlin-Reissner assumptions. Hinton and his colleagues [7-8] have presented a comprehensive study covering static and free vibration analyses of variable thickness prismatic folded plates and curved shells using linear, quadratic and cubic strips.

SSO techniques based on the finite element method have been used for many years with some success in the design of structures and structural components. Shape optimization of structures are modeled using two-dimensional representations was first investigated by Zienkiewicz and Campbell [9]. Since then much work has been reported. Hartman and Neumann [10] carried out shape optimization of a box girder bridge using the finite strip method with constraints on stresses and weight minimization as an objective. Hinton and Rao [11,12] investigated the optimum structural design of prismatic folded plate and shell structures using the finite strip method with strain energy minimization as an objective and allowed the cross sectional shape and thickness to be varied.

2 Mathematical Definition of Optimization Problem

The optimization problem may be summarized in the formal mathematical language of nonlinear programming as follows: Find the design vector s which maximizes (or minimizes) the objective function $F(s)$ subject to the behavioural constraints $g_j(s) \leq 0$, equality constraints $h_k(s) = 0$ and explicit geometric constraints $s_i^l \leq s_i \leq s_i^u$. The subscripts j , k and i denote the number of behavioural constraints, equality constraints and design variables respectively. The terms s_i^l and s_i^u refer to the specified lower and upper bounds on the design variables. [Table 1](#) summarizes the list of commonly used design variables, objective functions and inequality constraints in SSO.

Table 1: Design variables, objective functions & constraints used in structural shape optimization

<p>Design variables ‘s’</p> <ul style="list-style-type: none"> •Length of segments •Thickness of segments <p>Objective functions $F(s)$</p> <ul style="list-style-type: none"> •Weight minimization •Strain energy minimization <p>Constraint functions $g(s)$</p> <ul style="list-style-type: none"> •Stress constraint •Weight constraint
--

In general, the functions F , g_j and h_k may all be non-linear implicit function of the design variables s . The objective function is minimization of strain energy or weight, subject to stress or weight constraints. In addition, explicit geometrical constraints are imposed on the design variables to avoid impractical geometries. For example, a minimum element thickness is defined to avoid zero or 'negative' element thickness values. It is worth mentioning here that the objective function and the constraint hull may be non-convex and therefore local optima may exist.

3 Structural Shape Optimization Algorithm

The basic algorithm for structural shape optimization is given in [Figure 1](#).

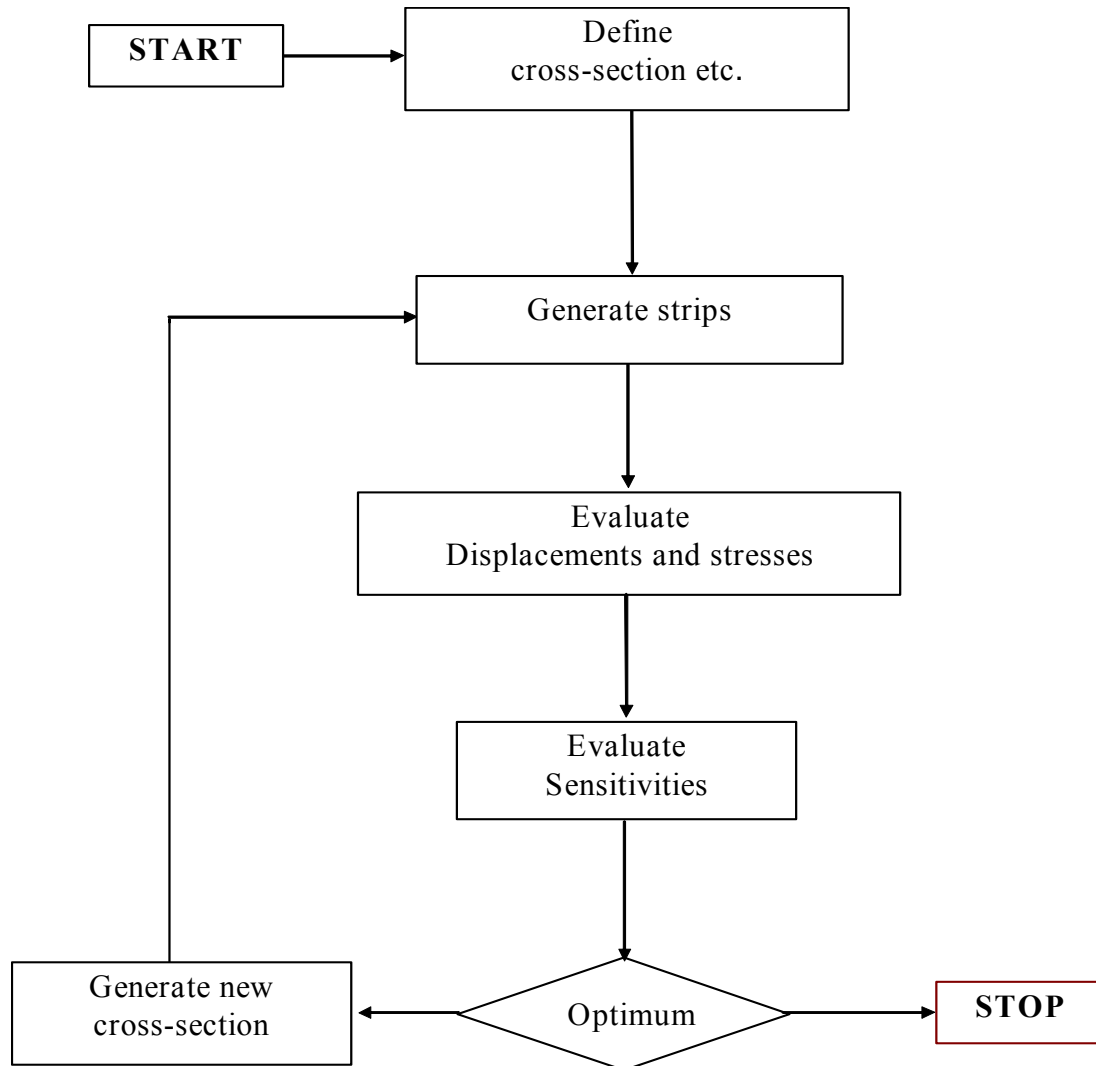


Figure 1 Basic approach to structural shape optimization.

A typical SSO procedure is based on the following algorithm:

1. The optimization problem, which includes the objective function, constraints, design variables, etc., are defined. The objective function and behavioral constraints are nonlinear implicit functions of the design variables.

2. The initial cross-section of the box girder bridge cross-section in terms of a set of design variables $\mathbf{s}^{(1)} = [s_1^{(1)}, s_2^{(1)}, \dots, s_n^{(1)}]^T$ are defined. Design variables may include the coordinates and the thickness at some specific points, and define the cross-sectional geometry. (The superscript denotes the design number in other words the optimization iteration number).
3. Suitable finite strips are generated. This may be achieved with an automatic mesh generator for a prescribed mesh density. In this study, only uniform mesh densities are used.
4. Displacements and stresses are evaluated. The finite strips analysis for current design $\mathbf{s}^{(c)}$ is then carried out and the displacements and stresses are evaluated together with the objective function and constraints. A feasible design variable vector $\mathbf{s}^{(1)}$ is usually used for initial designs but this is not always necessary.
5. The sensitivities of various items such as strain energy, displacements, stresses and the objective function of the current design to small changes in the design variables are evaluated. Methods for evaluating the sensitivities may be semi analytical or can be based on finite differences. In the present work, both methods are used.
6. Modify the current design and evaluate the design changes $\Delta s^{(c)}$ using the mathematical programming methods.
7. Check the new design changes $\Delta s^{(c)}$. If the design changes $\Delta s^{(c)}$ are non-zero then update the design vector to

$$\mathbf{s}^{(c+1)} = \mathbf{s}^{(c)} + \Delta \mathbf{s}^{(c)}$$

and a new cross-section is generated with an improved value of the objective function. The new geometry is sent to the mesh generator, which automatically generates a new analysis model, and the whole process is repeated from step 3. Otherwise stop.

4 Geometry Modelling

4.1 Structural shape definition

The definition and control of the geometric model of the structure to be optimized is a complex task. The cross-section of box girder bridge encountered in practice are so arbitrary and complex that it is essential that they should be presented in a convenient way using computer aided design tools, such as parametric cubic spline methods [13,14].

For the convenience we have adopted certain standard terms for the representation of the shape of the structure, which will be referred to frequently. The cross section of a typical box girder bridge structure is shown in [Figure 2](#). It is formed by an assembly of segments. Each segment is a cubic spline curve passing through certain *key points* all of which lie on the midsurface of the structure cross-section. Some key points are common to different segments at their points of intersection.

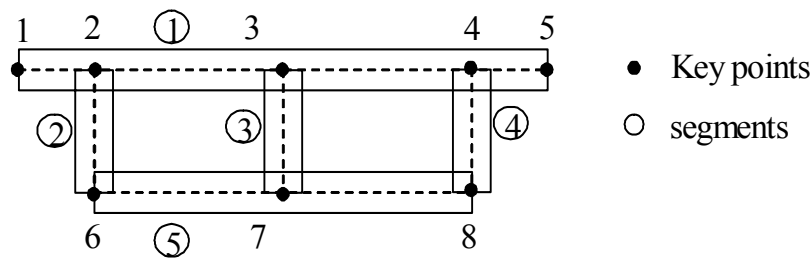


Figure 2 Geometric representation of box girder bridge

The *number of key points* used to define the shape of the structure is another important aspect in shape optimization. For curved segments, the more key points used the better the representation of the middle surface of the structure. However, it should be noted that in structural shape optimization procedures increasing the number of key points leads to an increase in the number of design variables and is likely to lead to greater computational expense.

By judicious linking of design variables at two or more key points, the length of a segment can be treated as a design variable and symmetry of shape can be easily achieved; and also, the number of design variables is considerably reduced.

4.2 Structural thickness definition

The thickness of the box girder bridge is specified at some or all of the key points of the structure and then interpolated using cubic splines or lower order functions this results in smooth structure shapes. By linking of thickness variables, piecewise constant or linear variations can be obtained; this is necessary in some cases such as box girders.

4.3 Selection of constraint points

In weight minimization it is necessary to constraint some function of the stresses (for example, the von Mises stress or principal stress) to be less than or equal to a certain specified value everywhere throughout the entire structure. In SSO procedures where re-meshing is performed at every iteration the function cannot be associated with the nodes since their number and position do not remain constant. Therefore, apart from being used to represent the shape and thickness, the key points are also used as stress sampling points to verify whether the stress constraint has been satisfied or not. Although this approach is satisfactory in most cases, it can be dangerous, since the maximum value of the stress may not occur at a key point. To avoid this potential problem, the points where the maximum stress occur are also taken as constraint points in addition to the key points. This approach has been found to be reliable.

4.4 Mesh generation

The next step is to generate a suitable finite strip mesh. This may be achieved with an automatic mesh generator for a prescribed mesh density. Mesh generation should be robust, versatile, and efficient. Here, we use a mesh generator, which incorporates a re-meshing facility to allow for the possibility of refinement. It also allows for a significant variation in mesh spacing throughout the region of interest. The mesh generator can generate meshes of two, three and four noded elements and strips. Moreover, the box girder bridge thickness is also interpolated from the key points to the nodal points using cubic splines.

To control the spatial distribution of strip sizes or mesh density throughout the domain, it is convenient to specify the mesh density at a sequence of points in the structure. The mesh density is a piecewise linear function of the values of mesh size δ at key points. At the initial stages of the analysis, mesh density values given at the two end key points of each segment will be sufficient if only a uniform or a linearly varying mesh density is required [14]. [Figure 3](#) shows a mesh of box girder bridge.

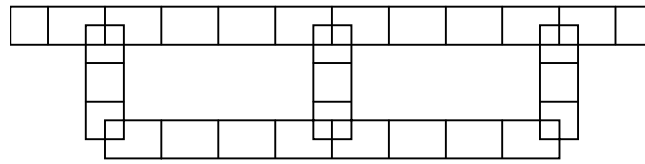


Figure 3 Mesh representation of box girder bridge

5 Structural Analysis

Box girder bridges with constant transverse cross-section with diaphragm ends are quite common. These structures are either of straight or curved planform and can have complex cross-sections. In some cases they may also rest on elastic foundations. Considerably research effort has been directed towards the development of accurate and inexpensive analysis procedures.

5.1 Theory of structural analysis and strip formulation

The finite strip method has proven to be an inexpensive and useful tool in analysis of structures having regular prismatic type geometry and simple boundary conditions. Structures which are simply supported on diaphragms at two opposite edges with the remaining edges arbitrarily restrained, and where the cross section does not change between the simply supported ends, can be analyzed accurately and inexpensively using the finite strip method in cases where a full finite element analysis could be considered extravagant. The structures can have rectangular or curved planforms. The finite strip method combines the use of Fourier expansions and one-dimensional finite elements to model the longitudinal and transverse structural behavior respectively.

5.1.1 Total potential energy

Consider the Mindlin-Reissner curved shell strip shown in [Figure 4](#). Displacement components u_ℓ, v_ℓ and w_ℓ are translation in the ℓ , η and n directions respectively. Note that η varies from an angle 0 to β along a curve of radius r .

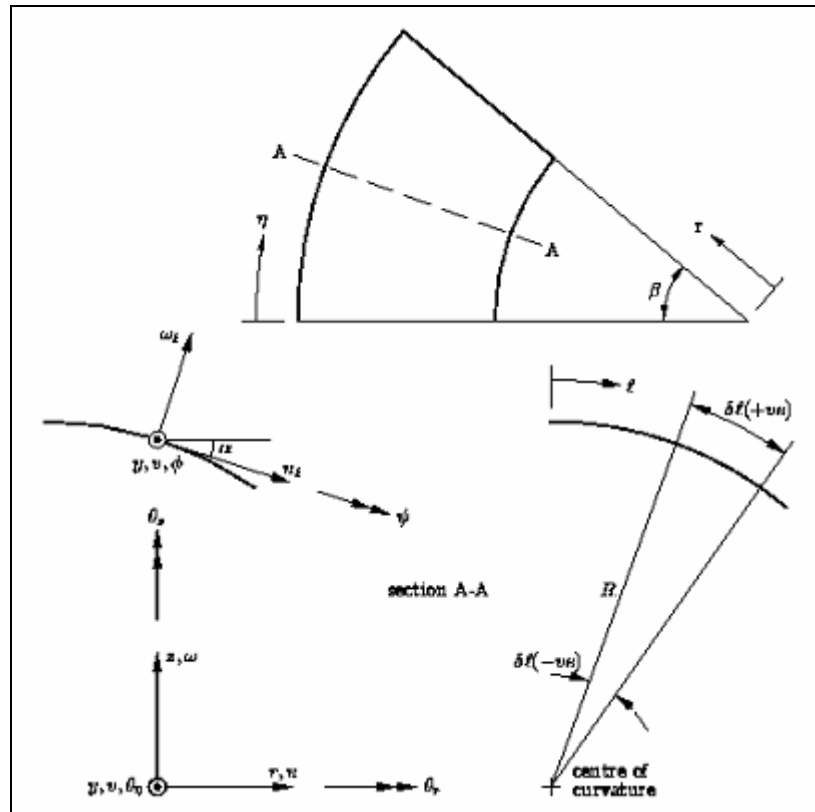


Figure 4. Definition of Mindlin-Reissner finite strips which are curved in plan.

The displacement components u_ℓ and w_ℓ may be written in terms of global displacements u and w in the r and z directions as

$$u_\ell = u \cos \alpha + w \sin \alpha$$

$$w_\ell = -u \sin \alpha + w \cos \alpha \quad (1)$$

where α is the angle between the r and ℓ axes; see [Figure 4](#). The radius of curvature R may be obtained from the expression

$$\frac{d\alpha}{d\ell} = -\frac{1}{R} \quad (2)$$

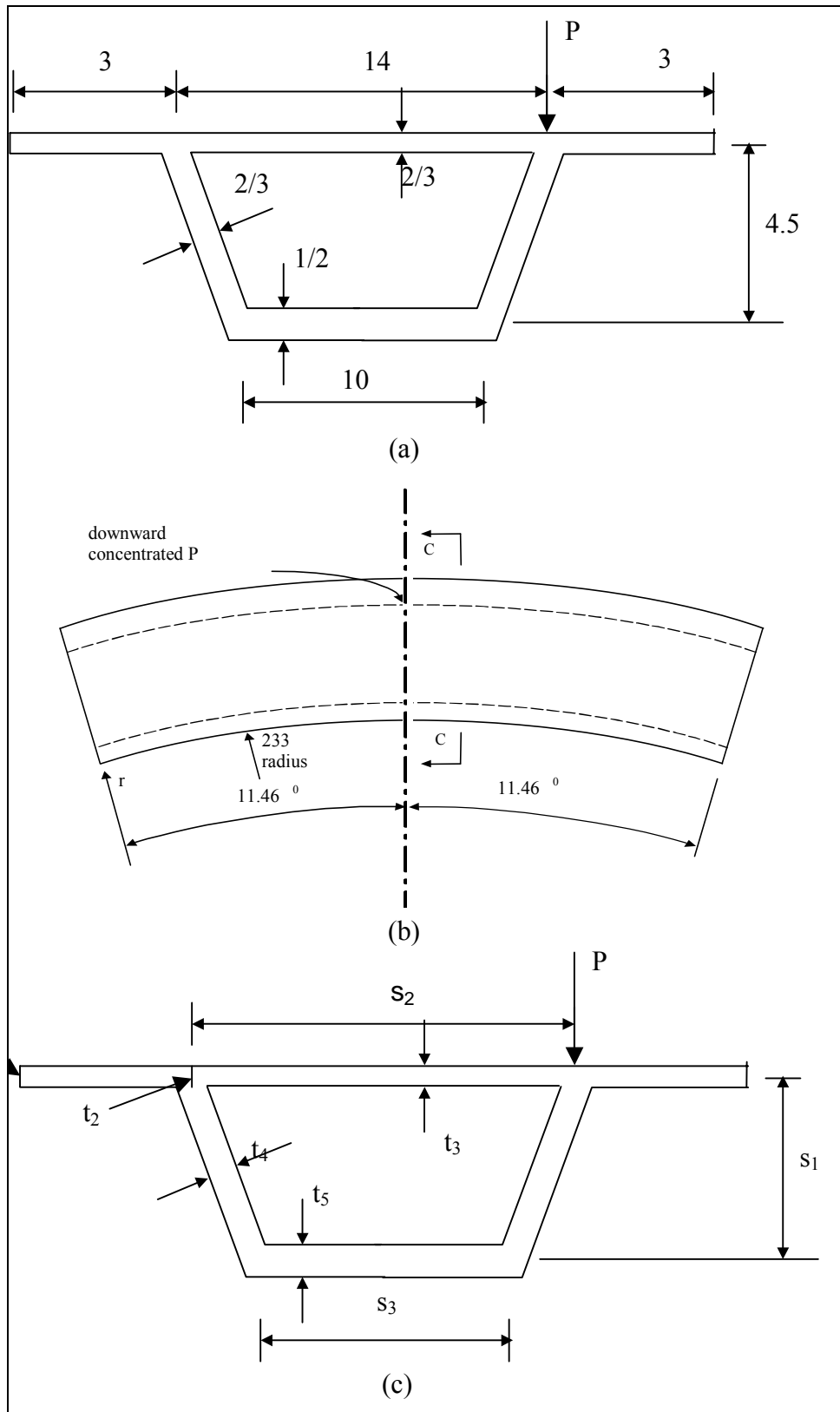


Figure 5 Single cell curved box girder bridge analyzed by Sisodiya and Ghali[22]

(a) cross-sectional view; (b) plan view, (c) position of design variables.

The total potential energy for a typical curved Mindlin-Reisner strip spanning over an angle β resting on an elastic Winkler-type foundation of modulus k is given in terms of the global displacements u, v, w and the rotations ϕ and ψ of the mid-surface normal in the ℓn and $\eta\eta$ planes respectively by the expressions [15]

$$I(u, v, w, \phi, \psi) = 1/2 \int_0^\beta \left([\boldsymbol{\epsilon}_m]^T \mathbf{D}_m \boldsymbol{\epsilon}_m + [\boldsymbol{\epsilon}_b]^T \mathbf{D}_b \boldsymbol{\epsilon}_b + [\boldsymbol{\epsilon}_s]^T \mathbf{D}_s \boldsymbol{\epsilon}_s + kw_\ell^2 \right) rd\ell d\eta - \int_0^\beta \int \mathbf{u}^T \mathbf{g} rd\ell d\eta - \int_0^\beta \bar{\mathbf{u}}^T \bar{\mathbf{g}} rd\eta \quad (3)$$

where $\boldsymbol{\epsilon}_m$, $\boldsymbol{\epsilon}_b$ and $\boldsymbol{\epsilon}_s$ are the membrane, bending or curvatures and transverse shear strains respectively and given in Table 2 for box girder bridge in curved planforms. Note that the method used to calculate the quantities are given in Hinton and Rao [8].

Table 2. Strain terms and strain-displacement matrices for curved in plan

$\boldsymbol{\epsilon}_m$	$\left[\frac{\partial u}{\partial \ell} \cos \alpha + \frac{\partial w}{\partial \ell} \sin \alpha, \left(u + \frac{\partial v}{\partial \eta} \right) / r, \left(\frac{\partial u}{\partial \eta} \cos \alpha + \frac{\partial w}{\partial \eta} \sin \alpha - v \cos \alpha \right) / r + \frac{\partial v}{\partial \ell} \right]^T$
$\boldsymbol{\epsilon}_b$	$\left[-\frac{\partial \phi}{\partial \ell}, -\left(\frac{\partial \psi}{\partial \eta} + \phi \cos \alpha \right) / r, \left(-\frac{\partial \phi}{\partial \eta} + \psi \cos \alpha + \frac{\partial v}{\partial \ell} \sin \alpha \right) / r - \frac{\partial \psi}{\partial \ell} + \frac{d\alpha}{d\ell} \left(\frac{\partial u}{\partial y} \cos \alpha + \frac{\partial w}{\partial y} \sin \alpha \right) / r \right]^T$
$\boldsymbol{\epsilon}_s$	$\left[-\frac{\partial u}{\partial \ell} \sin \alpha + \frac{\partial w}{\partial \ell} \cos \alpha - \phi, \left(-\frac{\partial u}{\partial \eta} \sin \alpha + \frac{\partial w}{\partial \eta} \cos \alpha + v \sin \alpha \right) / r - \psi \right]^T$
\mathbf{B}_m^p	$\begin{bmatrix} (dN_i/d\ell)S_p \cos \alpha & 0 & (dN_i/d\ell)S_p \sin \alpha & 0 & 0 \\ (N_i/r)S_p & -(\bar{p}N_i/r)S_p & 0 & 0 & 0 \\ (\bar{p}N_i/r)C_p \cos \alpha & (dN_i/d\ell - (N_i/r)\cos \alpha)C_p & (\bar{p}N_i/r)C_p \sin \alpha & 0 & 0 \end{bmatrix}$
\mathbf{B}_{bs}^p	$\begin{bmatrix} 0 & 0 & 0 & -(dN_i/d\ell)S_p & 0 \\ 0 & 0 & 0 & -(N_i/r)S_p \cos \alpha & (\bar{p}N_i/r)S_p \\ (\bar{p}(N_i/r)C_p \cos \alpha)/R & dN_i/d\ell(1/r)C_p \sin \alpha & (\bar{p}(N_i/r)C_p \sin \alpha)/R & -(\bar{p}N_i/r)C_p & ((N_i/r)\cos \alpha - dN_i/d\ell)C_p \end{bmatrix}$
\mathbf{B}_{si}^p	$\begin{bmatrix} -(dN_i/d\ell)S_p \sin \alpha & 0 & (dN_i/d\ell)S_p \cos \alpha & -N_i S_p & 0 \\ -(\bar{p}N_i/r)C_p \sin \alpha & (N_i/r)C_p \sin \alpha & (\bar{p}N_i/r)C_p \cos \alpha & 0 & -N_i C_p \end{bmatrix}$

For an isotropic material of elastic modulus E , Poisson's ratio ν and thickness t , the matrix of membrane, flexural and shear rigidities have the form

$$\mathbf{D}_m = \frac{Et}{(1-\nu^2)} \begin{bmatrix} 1 & \nu & 0 \\ \nu & 1 & 0 \\ 0 & 0 & (1-\nu)/2 \end{bmatrix} \quad \mathbf{D}_b = \frac{Et^3}{12(1-\nu^2)} \begin{bmatrix} 1 & \nu & 0 \\ \nu & 1 & 0 \\ 0 & 0 & (1-\nu)/2 \end{bmatrix}$$

$$\mathbf{D}_s = \frac{\kappa Et}{2(1+\nu)} \begin{bmatrix} 1 & 0 \\ 0 & 1 \end{bmatrix} \quad (4)$$

where κ is the shear modification factor and is usually taken as 5/6 for an isotropic material. Note that the displacement components \mathbf{u} are listed as

$$\mathbf{u} = [u, v, w, \phi, \psi]^T \quad (5)$$

and the corresponding distributed loadings \mathbf{g} may be written as

$$\mathbf{g} = [g_u, g_v, g_w, g_\phi, g_\psi]^T \quad (6)$$

The distributed line loadings are

$$\bar{\mathbf{g}} = [\bar{F}_u, \bar{F}_v, \bar{F}_w, \bar{F}_\phi, \bar{F}_\psi]^T \quad (7)$$

in which the line forces are \bar{F}_u and \bar{F}_v and \bar{F}_w and the distributed line couples are \bar{F}_ϕ and \bar{F}_ψ .

These loadings are applied at $\ell = \bar{\ell}$ where the corresponding displacements are

$$\bar{\mathbf{u}} = [\bar{u}, \bar{v}, \bar{w}, \bar{\phi}, \bar{\psi}]^T \quad (8)$$

5.1.2 Finite strip idealization

Using n -noded, $C(0)$ strips, the global displacements and rotations may be interpolated within each strip by the expressions

$$\begin{aligned} u(\ell, \eta) &= \sum_{p=1}^h u^p(\ell) S_p; & v(\ell, \eta) &= \sum_{p=1}^h v^p(\ell) C_p \\ w(\ell, \eta) &= \sum_{p=1}^h w^p(\ell) S_p; & \phi(\ell, \eta) &= \sum_{p=1}^h \phi^p(\ell) S_p \\ \psi(\ell, \eta) &= \sum_{p=1}^h \psi^p(\ell) C_p \end{aligned} \quad (9)$$

where $C_p = \cos(p\pi\eta/b)$ and $S_p = \sin(p\pi\eta/b)$ and u^p, v^p, w^p, ϕ^p and ψ^p are displacement and rotation amplitudes for the p^{th} harmonic term and h is the number of harmonic terms used in the analysis.

The next step is to discretize the displacement and rotation amplitudes (which are functions of the ℓ -coordinate only) using an n -noded finite element representation so that within a strip e the amplitudes can be written as

$$\begin{aligned} u^p(\ell) &= \sum_{i=1}^n N_i u_i^p; & v^p(\ell) &= \sum_{i=1}^n N_i v_i^p; & w^p(\ell) &= \sum_{i=1}^n N_i w_i^p \\ \phi^p(\ell) &= \sum_{i=1}^n N_i \phi_i^p; & \psi^p(\ell) &= \sum_{i=1}^n N_i \psi_i^p \end{aligned} \quad (10)$$

where u_i^p , v_i^p , w_i^p , ϕ_i^p and ψ_i^p are typical nodal degrees of freedom associated with node i and harmonic p . For convenience, these terms are grouped together so that

$$\mathbf{d}_i^p = [u_i^p, v_i^p, w_i^p, \phi_i^p, \psi_i^p]^T \quad (11)$$

$N_i(\xi)$, is the shape function associated with node i [8]. These elements are essentially isoperimetric so that

$$r = \sum_{i=1}^n N_i r_i; \quad z = \sum_{i=1}^n N_i z_i; \quad t = \sum_{i=1}^n N_i t_i \quad (12)$$

where r_i and z_i are typical coordinates of node i and t_i is the thickness at node i . Note also that the Jacobian is

$$J = \frac{d\ell}{d\xi} = \left[\left(\frac{dr}{d\xi} \right)^2 + \left(\frac{dz}{d\xi} \right)^2 \right]^{1/2}; \quad d\ell = J d\xi \quad (13)$$

where

$$\frac{dr}{d\xi} = \sum_{i=1}^n \frac{dN_i}{d\xi} r_i; \quad \frac{dz}{d\xi} = \sum_{i=1}^n \frac{dN_i}{d\xi} z_i. \quad (14)$$

Also, it is possible to write

$$\sin \alpha = \frac{dz}{d\xi} \frac{1}{J}; \quad \cos \alpha = \frac{dr}{d\xi} \frac{1}{J} \quad (15)$$

and

$$\frac{dN_i}{d\ell} = \frac{dN_i}{d\xi} \frac{1}{J}. \quad (16)$$

The membrane strains $\boldsymbol{\varepsilon}_m$, flexural strain or curvatures $\boldsymbol{\varepsilon}_b$ and transverse shear strain $\boldsymbol{\varepsilon}_s$ may then be expressed as

$$\boldsymbol{\varepsilon}_m = \sum_{p=1}^h \sum_{i=1}^n \mathbf{B}_{mi}^p \mathbf{d}_i^p \quad \boldsymbol{\varepsilon}_b = \sum_{p=1}^h \sum_{i=1}^n \mathbf{B}_{bi}^p \mathbf{d}_i^p \quad \boldsymbol{\varepsilon}_s = \sum_{p=1}^h \sum_{i=1}^n \mathbf{B}_{si}^p \mathbf{d}_i^p \quad (17)$$

and \mathbf{B}_{mi}^p , \mathbf{B}_{bi}^p and \mathbf{B}_{si}^p are the membrane, bending and shear strain displacement matrices associated with harmonic p , node i and Jacobian J and given in [Table 2](#).

where if we set $\bar{p} = p\pi / \beta$. Note that the method for evaluating R is given in [8].

The loads acting over the structure are expanded in the same way as the displacements, that is as the sum of the harmonic series along the length of the structure, so that

$$g_u(\ell, \eta) = \sum_{p=1}^h g_u^p(\ell) S_p; \quad g_v(\ell, \eta) = \sum_{p=1}^h g_v^p(\ell) C_p;$$

$$g_w(\ell, \eta) = \sum_{p=1}^h g_w^p(\ell) S_p; \quad g_\phi(\ell, \eta) = \sum_{p=1}^h g_\phi^p(\ell) S_p;$$

$$g_{\psi}(\ell, \eta) = \sum_{p=1}^h g_{\psi}^p(\ell) C_p ; \quad (18)$$

The next step is to discretize the load amplitudes (which are functions of the ℓ -coordinate only) using a standard finite element representation so that within a strip e the amplitudes can be written as

$$g_u^p(\ell) = \sum_{i=1}^n N_i g_{ui}^p ; \quad g_v^p(\ell) = \sum_{i=1}^n N_i g_{vi}^p ; \quad g_w^p(\ell) = \sum_{i=1}^n N_i g_{wi}^p$$

$$g_{\phi}^p(\ell) = \sum_{i=1}^n N_i g_{\phi i}^p ; \quad g_{\psi}^p(\ell) = \sum_{i=1}^n N_i g_{\psi i}^p \quad (19)$$

where, for example, g_{ui}^p is the value of $g_u^p(\ell)$ at node i . The nodal load amplitudes are calculated individually using Euler's formula. The consistent nodal force vector $\{\mathbf{f}_i^e\}^p$ associated with node i and harmonic p is written as

$$\{\mathbf{f}_i^e\}^p = [f_{ui}^p, f_{vi}^p, f_{wi}^p, f_{\phi i}^p, f_{\psi i}^p]^T \quad (20)$$

The expressions for the consistent nodal force vector for different load cases can be easily evaluated and are presented in [8].

Thus, neglecting line loads and couples, the contribution to the total potential from strip e may be expressed as

$$I^e = 1/2 \sum_{i=1}^n \sum_{j=1}^n \sum_{p=1}^n \sum_{q=1}^n [\{\mathbf{d}_i^e\}]^T [\mathbf{K}_{ij}^e]^{pq} \{\mathbf{d}_j^e\}^q - \sum_{i=1}^n \sum_{p=1}^h [\{\mathbf{d}_i^e\}^p]^T \{\mathbf{f}_i^e\}^p \quad (21)$$

where the sub matrix of the strip stiffness matrix $[\mathbf{K}_{ij}^e]^{pq}$ linking nodes i and j and harmonics p and q has the form

$$[\mathbf{K}_{ij}^e]^{pq} = \int_0^{\beta} \int_{-1}^{+1} \{[B_{mi}^p]^T D_m B_{mj}^q + [B_{bi}^p]^T D_b B_{bj}^q + [B_{si}^p]^T D_s B_{sj}^q\} r J d\xi d\eta + [\bar{\mathbf{K}}_{ij}^e]^{pq} \quad (22)$$

where

$$[\bar{\mathbf{K}}_{ij}^e]^{pq} = \begin{bmatrix} k_{uu} & 0 & k_{uw} & 0 & 0 \\ 0 & 0 & 0 & 0 & 0 \\ k_{wu} & 0 & k_{ww} & 0 & 0 \\ 0 & 0 & 0 & 0 & 0 \\ 0 & 0 & 0 & 0 & 0 \end{bmatrix} \quad (23)$$

in which

$$k_{uu} = (\beta/2) \int_{-1}^{+1} k N_i N_j (\sin^2 \alpha) r J d\xi$$

$$k_{uw} \text{ and } k_{wu} = -(\beta/2) \int_{-1}^{+1} k N_i N_j (\sin \alpha \cos \alpha) r J d\xi$$

$$k_{ww} = (\beta/2) \int_{-1}^{+1} k N_i N_j (\cos^2 \alpha) r J d\xi \quad (24)$$

Note that $[\bar{\mathbf{K}}_{ij}^e]^{pq}$ does not depend on p or q and that $[\mathbf{K}_{ij}^e]^{pq}$ and $[\bar{\mathbf{K}}_{ij}^e]^{pq} = \mathbf{0}$ if $p \neq q$ because of the orthogonality conditions [8]. To avoid locking behavior, reduced integration is adopted i.e. one, two and three point Gauss-Legendre Quadrature is used for the two, three and four noded strips respectively. Note also that since the rigidities \mathbf{D}_m , \mathbf{D}_b and \mathbf{D}_s all depend on t and since t is interpolated within each strip e from the nodal value t_i , strip of variable thickness may be easily accommodated in the present formulation.

5.1.3 Stress resultants and strain energy evaluation

The stress resultant vector for harmonic p can be expressed as

$$\boldsymbol{\sigma}^p = \begin{bmatrix} \boldsymbol{\sigma}_m^p \\ \boldsymbol{\sigma}_b^p \\ \boldsymbol{\sigma}_s^p \end{bmatrix} \quad (25)$$

where $\boldsymbol{\sigma}_m^p$, $\boldsymbol{\sigma}_b^p$ and $\boldsymbol{\sigma}_s^p$ are the stress resultants vectors due to membrane, bending and shear effect, so that

$$\boldsymbol{\sigma}_m^p = [N_\ell, N_y, N_{\ell y}]^T \quad \boldsymbol{\sigma}_b^p = [M_\ell, M_y, M_{\ell y}]^T \quad \boldsymbol{\sigma}_s^p = [Q_\ell, Q_y]^T \quad (26)$$

These stress resultants can be obtained by the expressions

$$\begin{aligned} \boldsymbol{\sigma}_m^p &= \mathbf{D}_m \sum_{p=1}^h \sum_{i=1}^n \mathbf{B}_{mi}^p \mathbf{d}_i^p & \boldsymbol{\sigma}_b^p &= \mathbf{D}_b \sum_{p=1}^h \sum_{i=1}^n \mathbf{B}_{bi}^p \mathbf{d}_i^p \\ \boldsymbol{\sigma}_s^p &= \mathbf{D}_s \sum_{p=1}^h \sum_{i=1}^n \mathbf{B}_{si}^p \mathbf{d}_i^p. \end{aligned} \quad (27)$$

For a typical strip, the strain energy for p harmonic due to bending, membrane and shear can be evaluated by the expressions

$$\begin{aligned} \|\mathbf{W}\|_b^2 &= \int_0^\beta \int_{-1}^1 [\boldsymbol{\sigma}_b^p]^T \mathbf{D}_b^{-1} \boldsymbol{\sigma}_b^p r J d\xi d\eta, \\ \|\mathbf{W}\|_m^2 &= \int_0^\beta \int_{-1}^1 [\boldsymbol{\sigma}_m^p]^T \mathbf{D}_m^{-1} \boldsymbol{\sigma}_m^p r J d\xi d\eta \\ \|\mathbf{W}\|_s^2 &= \int_0^\beta \int_{-1}^1 [\boldsymbol{\sigma}_s^p]^T \mathbf{D}_s^{-1} \boldsymbol{\sigma}_s^p r J d\xi d\eta \end{aligned} \quad (28)$$

since we have the orthogonality conditions. The accumulated contributions to the bending, membrane and shear energies are obtained by summing the contributions from each strip. The total strain energy of the finite strip solution $\|\mathbf{W}\|^2$ is then computed using the expression

$$\|\mathbf{W}\|^2 = \|\mathbf{W}\|_b^2 + \|\mathbf{W}\|_m^2 + \|\mathbf{W}\|_s^2. \quad (29)$$

5.1.4 Branched strips

In the case of plates and smooth shells, the strips all lie in the same plane, which coincides with the strip middle surface, whereas for branched structures the strips meet at different angles. Thus, to assemble the complete stiffness matrix for branched shell structures, displacements must be expressed in a common and uniquely defined coordinate system. The translational degrees of freedom u_i , v_i and w_i are already expressed in the global x , y and z directions and therefore the associated stiffness terms do not require any further transformation. However,

rotation degrees of freedom ψ_i are related to the local axis ℓ and therefore the associated stiffness terms must be transformed accordingly. Thus it is possible to write

$$\mathbf{d}_i^p = \mathbf{T} \bar{\mathbf{d}}_i^p \quad \mathbf{f}_i^p = \mathbf{T} \bar{\mathbf{f}}_i^p \quad (30)$$

where

$$\bar{\mathbf{d}}_i^p = [u_i^p, v_i^p, w_i^p, \theta_{ri}^p, \theta_{\eta i}^p, \theta_{zi}^p]^T \quad \text{and} \quad (31)$$

$$\bar{\mathbf{f}}_i^p = [f_{ui}^p, f_{vi}^p, f_{wi}^p, f_{\theta ri}^p, f_{\theta \eta i}^p, f_{\theta zi}^p]^T$$

are the displacement and force vector at node i of strip e . The matrix \mathbf{T} can now be defined as

$$\mathbf{T} = \begin{bmatrix} 1 & 0 & 0 & 0 & 0 & 0 \\ 0 & 1 & 0 & 0 & 0 & 0 \\ 0 & 0 & 1 & 0 & 0 & 0 \\ 0 & 0 & 0 & 0 & 1 & 0 \\ 0 & 0 & 0 & \cos \alpha & 0 & \sin \alpha \end{bmatrix} \quad (32)$$

Note that $\phi_i = \theta_{yi}$. The membrane strain displacement matrix is then modified to

$$\bar{\mathbf{B}}_{mi} = \mathbf{B}_{mi} \mathbf{T} \quad (33)$$

with similar expressions for $\bar{\mathbf{B}}_{bi}$ and $\bar{\mathbf{B}}_{si}$. The stiffness and mass matrices can be written as

$$[\mathbf{K}_{ij}^e]^{pp} = \int_0^{\beta} \int_{-1}^1 \{ [\bar{\mathbf{B}}_{mi}^p]^T \mathbf{D}_m \bar{\mathbf{B}}_{mj}^q + [\bar{\mathbf{B}}_{bi}^p]^T \mathbf{D}_b \bar{\mathbf{B}}_{bj}^q + [\bar{\mathbf{B}}_{si}^p]^T \mathbf{D}_s \bar{\mathbf{B}}_{sj}^q \} r J d\xi d\eta$$

$$+ [\mathbf{T}]^T [\bar{\mathbf{K}}_{ij}^{pp}] \mathbf{T} \quad (34)$$

6 Sensitivity Analysis

Having completed the finite strip analysis, we now evaluate the sensitivities of the current design to small changes in the design variables. We calculate the sensitivities of the strain energy. Methods for evaluating the sensitivities may be purely analytical or can be based on finite differences in which case the choice of the step size may be crucial. Alternatively, we may use semi-analytical methods, which are partly analytical and partly based on finite differences.

Sensitivity analysis consists of the systematic calculation of the derivatives of the response of the finite strip model with respect to parameters characterizing the model i.e. the design variables, which may be length, thickness or shape. Finite strip structural analysis programs are used to calculate the response quantities such as displacements, stresses, etc. The first partial derivatives of the structural response quantities with respect to the shape (or other) variables provide the essential information required to couple mathematical programming methods and structural analysis procedures. The sensitivities provide the mathematical programming algorithm with search directions for optimum solutions.

In the present study, both the finite difference and semi analytical methods are used to calculate sensitivities. The finite difference method uses a difference formula to numerically approximate the derivatives. The semi-analytical method, which was originally proposed, by Zienkiewicz and Campbell [9] is quite popular in shape optimization and it combines the analytical and finite difference methods. The derivatives of some quantities are evaluated using finite difference whereas for the others the analytical method is adopted. These two methods are accurate,

computationally efficient and sensitive to round off and truncation errors associated with step size.

6.1 Derivative of displacements and stress resultants

To get $\partial \mathbf{d} / \partial s_i$ and $\partial \boldsymbol{\sigma} / \partial s_i$ the global finite difference method is used and the following expressions may be written

$$\frac{\partial \mathbf{d}}{\partial s_i} \approx \frac{\mathbf{d}(s_i + \Delta s_i) - \mathbf{d}(s_i)}{\Delta s_i} \quad (35)$$

$$\frac{\partial \boldsymbol{\sigma}}{\partial s_i} \approx \frac{\boldsymbol{\sigma}(s_i + \Delta s_i) - \boldsymbol{\sigma}(s_i)}{\Delta s_i} \quad (36)$$

where Δs_i is step size, $\mathbf{d}(s_i + \Delta s_i)$ is evaluated by solving

$$\mathbf{K}(s_i + \Delta s_i) \mathbf{d}(s_i + \Delta s_i) = \mathbf{f}(s_i + \Delta s_i) \quad (37)$$

and $\boldsymbol{\sigma}(s_i + \Delta s_i)$ is found from

$$\boldsymbol{\sigma}(s_i + \Delta s_i) = \mathbf{D}(s_i + \Delta s_i) \mathbf{B}(s_i + \Delta s_i) \mathbf{d}(s_i + \Delta s_i) \quad (38)$$

6.2 Derivative of volume

The volume derivative is calculated using a forward finite difference approximation

$$\frac{\partial V}{\partial s_i} \approx \frac{V(s_i + \Delta s_i) - V(s_i)}{\Delta s_i} \quad (39)$$

where the volume V of the whole structure (or cross-sectional area of the structure may also be used) can be calculated by adding the volumes of numerically integrated FSs.

7 Mathematical Programming

Nonlinear programming techniques are the most popular and widely used methods for structural optimization. Using the information derived from the analysis and design sensitivities, mathematical programming methods such as sequential quadratic programming or the Method of Moving Asymptotes (MMA) are used to generate shapes with improved objective function values. In the present work only the MMA algorithm [16] is used. No effort has been made to study the mathematical programming methods used for SSO procedures and the MMA algorithm is used here essentially as a 'black box'. The MMA method has the advantages in the early stages of the optimization to get close to the optimum in a fast and efficient manner, and SQP method exploits the higher accuracy of the to converge to the optimum.

8 Examples

Several box girder bridges curved in planform for which solutions are available have been analyzed. Note that in all cases the structures have simply supported end conditions at $\theta = 0$ and $\theta = \beta$ and only meshes with uniform spacings are considered. In the paper dimensions and units are given according to appropriate references. The units are consistent in all the examples.

The box girder bridge is optimized for the following objective function and constraints cases:

Strain energy minimization with a constraint that the total material volume of the structure should remain constant and Volume (or weight) minimization subject to the constraint that the maximum von-Mises stress should not exceed 5 % of its initial value prior to optimization.

In this paper only linear elastic behavior is considered and the optimized shape and thickness distributions are not checked for buckling under the given set of loads. Although some of the optimal shapes of the structures obtained may look impractical, they could serve as a guide to designing practical shapes and as an educational tool.

8.1 Single cell curved box girder bridge

In the first example a single cell curved box girder bridge analyzed by Sisodiya and Ghali [17] is considered. The geometry of the structure is shown in Figure 5 (a), (b). The bridge spans over an angle of $\alpha = 0.4 \text{ rad}$ with an inner radius of $r_0 = 233$. The following material properties are assumed: elastic modulus $E = 1 \text{ kip/in}^2$ and Poisson's ratio $\nu = 0.15$. The box girder is analyzed for a concentrated vertical load of intensity 1 kip at midspan applied above the outer web

Discussion of analysis results: using 26 odd harmonics and 17 cubic strips carries out the analyses. The results for the deflections and maximum stress resultants for the box girder are summarized in Table 3 and Table 4 for various number of harmonics and compare well with those presented using the finite element method by Sisodiya and Ghali [17].

Table 3 Comparison of deflections for single cell box girder bridge

number of harmonics	deflection w (in)	
	under the point	at the inner web
11	278.1	219.4
51	279.5	219.4
101	279.8	219.4
151	279.1	219.3
Ghali (FE/FS)	288.9	221.0

Table 4 Maximum stress resultants under point load at midspan

stresses $\times 10^{-2}$ kips/ft	Ref [22]	present
M_η	3.65	3.6468
M_r	2.75	2.711
N_η	40.50	40.720

Discussion of optimization results: The cross-sectional shape of the box girder bridge is defined using six segments and six key points. The location of the design variables and position of point load are shown in Figure 5(c). Three shape and five thickness design variables are considered.

Table 5 presents initial and optimal energies. Table 6 presents the initial and optimal design variables together with their bounds. For case (a) the problem of SE minimization 74.6 percent decrease and for case (b) the problem of volume minimization 44.5 percent decrease is obtained.

Table 5 Single cell curved box girder bridge: initial and optimal energies

	volume	total SE×10 ⁻⁴	% contributions to SE		
			membrane	bending	shear
initial	2420.303	2.7944	98.614	1.359	0.027
case (a)	----	0.7089	98.886	1.064	0.050
case (b)	1343.463	---	98.810	1.179	0.011

Table 6 Single cell curved box girder bridge: values of the design variables

Type	design variables			opt. design variables	
	max.	min.	initial	case (a)	case (b)
s ₁	9.000	2.250	4.500	9.000	8.086
s ₂	28.000	7.000	14.000	7.000	7.000
s ₃	20.000	5.000	10.000	9.262	5.936
t ₁	1.334	0.334	0.667	0.334	0.334
t ₂	1.334	0.334	0.667	0.334	0.354
t ₃	1.334	0.334	0.667	0.646	0.334
t ₄	1.334	0.334	0.667	0.427	0.334
t ₅	1.000	0.250	0.500	0.897	0.291

8.2 Two cell curved box girder bridge

This example involves the analysis of a two cell curved box girder bridge analyzed by Cheung and Cheung [18]. The geometry of the structure is shown in Figure 6 (a), (b). The bridge spans over an angle of $\alpha = 1.0 \text{ rad}$ with an inner radius of $r_0 = 78$. The following material properties are assumed: elastic modulus $E = 1 \text{ kip/in}^2$ and Poisson's ratio $\nu = 0.16$. Three separate load cases are considered: vertical load at midspan of intensity 1 kip is applied above (a) the inner web, (b) the middle of the top flange and (c) the outer web.

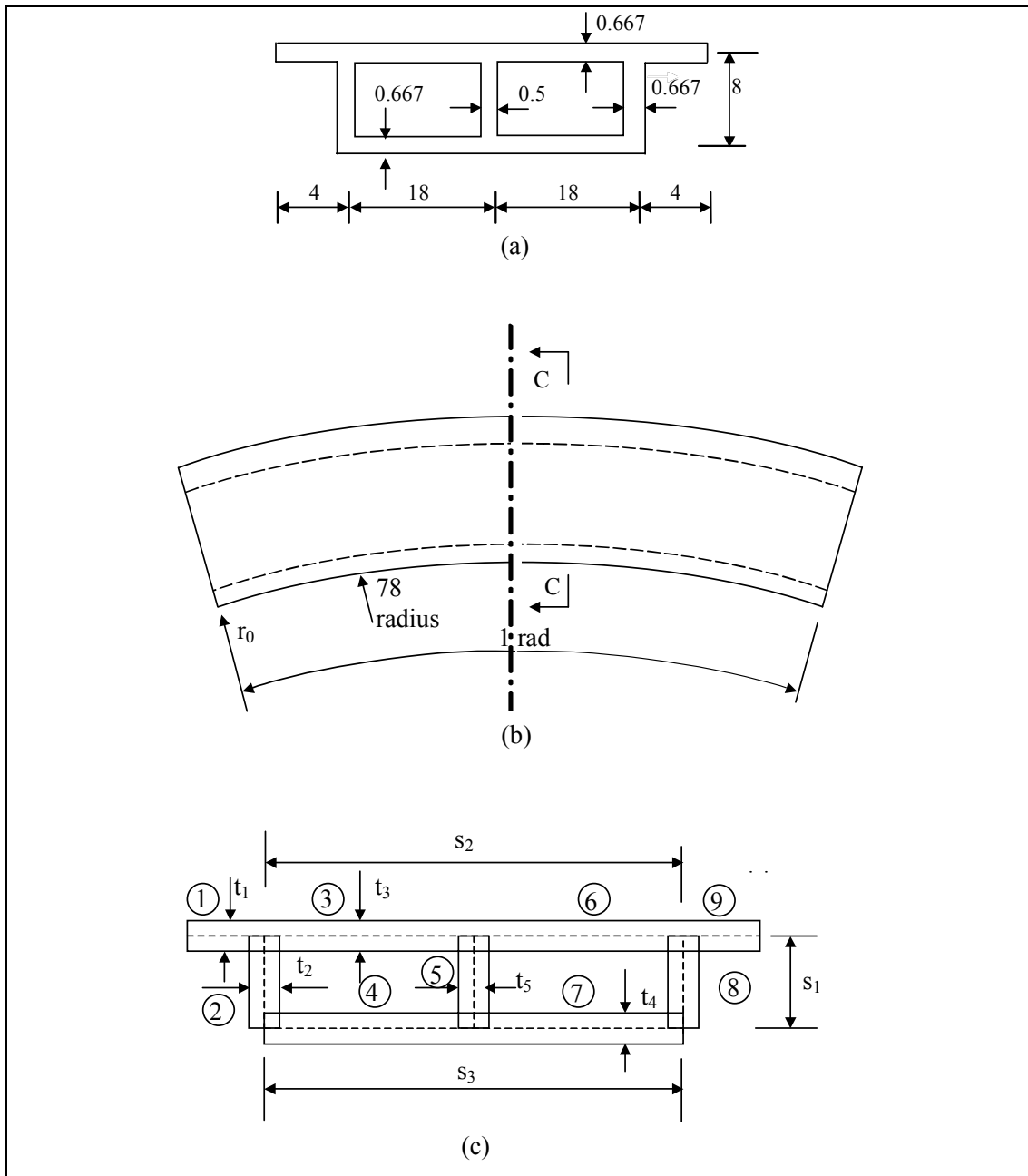


Figure 6 Two cell curved box girder bridge. (a) cross sectional view; (b) plan view. (All dimensions are ft), c) position of design variables.

Discussion of analysis results: The analyses are carried out using 15 odd harmonics. [Table 7](#) contains the magnitude of the SE and its composition. It can be noted that the membrane energy contribution increases as the point of application of the load changes from the inner web to the outer web. [Table 8](#) shows the deflections at mid-span and under point load. The deflections of two cell curved box girder bridge is compared with two different references. A good comparison is obtained with [\[15,18\]](#). [Table 9](#) compares the maximum stress resultants with [\[15,18\]](#) similar distribution of the stress resultants were obtained.

Table 7 Comparison of strain energy values for two cell curved box girder

loading position	$\ \mathbf{W}\ ^2 \text{ kip.in}$		% contributions to SE					
			membrane		bending		shear	
above	Ref	present	Ref	present	Ref	present	Ref	present
inner	71.86	71.86	67.7	67.69	32.0	32.02	0.3	0.29
middle	57.79	57.78	85.5	85.57	14.3	14.30	0.2	1.13
outer web	78.10	78.07	94.7	94.72	5.2	5.23	0.1	0.05

Table 8 Comparisons of deflections for two cell curved box girder under point load

Loading position above	deflection w (in)			
	18 linear strip		37 cubic strip	
	ref [21]	present	ref [23]	present
inner web	70.62	68.77	71.86	71.86
middle web	56.88	56.95	57.79	57.79
outer web	77.69	78.69	78.10	78.07

Table 9 Comparisons of maximum stress resultants for two cell curved box girder (reference values are approximately taken from graphics)

loading position	$M_n \times 10^{-2} \text{ kips.ft}$			$M_r \times 10^{-2} \text{ kips.ft}$			$N_n \times 10^{-1} \text{ kips/ft}$		
	Ref	Ref	present	Ref	Ref	present	Ref	Ref	present
inner	2.2	2.0	2.1	2.8	3.5	3.4	2.6	2.8	2.9
middle	1.9	1.9	1.8	2.1	2.7	2.7	1.3	1.6	1.6
outer	1.3	1.3	1.2	1.5	1.9	1.8	2.1	2.3	2.4

Discussion of optimization results: Optimization is done under the load is applied two points with an intensity of $P = 1 \text{ kip}$, at point A, on the top flange which is above inner web, and at point B, on the top flange which is above middle web (middle point of top flange).

The cross-sectional shape of the box girder bridge is modeled using nine segments and eight key points. The location of the design variables is shown in [Figure 6\(c\)](#). Shape design variables are the length of segment 2 and the total length of segment 3-6 and 4-7. Thickness design variables are the thickness of the top flange cantilever segments, the top and bottom flanges, and the middle and outer webs. Note that to maintain the symmetry, the length of segment 2 is forced to equal the lengths of the segments 5 and 8 by linking. Optimization is carried out for both shape design variables s_1, s_2 and s_3 and thickness design variables t_1, t_2, t_3, t_4 and t_5 together.

[Table 10](#) presents the initial and optimal design variables together with their bounds. [Table 11](#) presents initial and optimal energies. For case (a) the problem of SE minimization 62.2, 65.5 percent decreases and for case (b) the problem of volume minimization 28.6, 40.3 percent decreases are obtained when load is applied above point A and B respectively.

Table 10. Two cell curved box girder bridge: values of the design variables

design variables				Opt. design variables			
type	max.	min.	initial	point load (A)		point load (B)	
				case (a)	case (b)	case (a)	case (b)
s ₁	16.000	4.000	8.000	16.000	11.776	16.000	16.000
s ₂	72.000	18.000	36.000	36.070	55.619	18.000	36.040
s ₃	72.000	18.000	36.000	18.000	18.000	39.630	29.998
t ₁	1.334	0.334	0.667	0.334	0.334	0.334	0.334
t ₂	1.334	0.334	0.667	0.828	0.334	0.334	0.334
t ₃	1.334	0.334	0.667	0.334	0.334	0.825	0.334
t ₄	1.334	0.334	0.667	0.104	0.334	0.392	0.334
t ₅	1.000	0.250	0.500	0.250	0.447	1.000	0.313

Table 11. Two cell curved box girder bridge: initial and optimal energies

load	shape	volume	total SE×10 ⁻⁵	% contributions to SE		
				membrane	bending	shear
(A)	initial	6803.2	7.153	67.639	32.085	0.276
	case (a)	----	2.703	74.113	25.693	0.194
	case (b)	4855.97	---	74.966	24.959	0.074
(B)	initial	6803.2	5.740	85.598	14.289	0.113
	case (a)	----	1.979	88.387	11.511	0.102
	case (b)	4060.54	---	94.976	5.008	0.016

9 Conclusion

In the present work computational tools have been developed for geometric modeling, automatic mesh generation, analysis and shape optimization of box girder bridges. Several examples have been studied and used to test and to demonstrate the capabilities offered by this computational tool. Based on the above studies the following general conclusions can be drawn.

- Finite strip elements of the types presented in the present work, which can perform well in *curved* situations and *thick*, *thin* and *variable thickness* cases have proved to be most appropriate for the analysis and optimization of box girder structures due to their inexpensiveness, accuracy and reliability.
- The results obtained using finite strips analysis tools generally compare well with those obtained from other sources based on alternative formulations such as thin beam theory, shell theories. The results illustrate that the finite strip methods presented here can be used with confidence for the static analysis of box girder bridges, which has curved planforms.

- The objective functions and constraint functions implemented in the program allow the design of a wide range of box girder bridge for curved in plan.
- Shape optimization with a strain energy minimization as the objective seems to be a mathematically better-behaved problem than those defined using volume/weight minimization as objective function.
- The more accurate the information given to the optimizer, the faster the convergence achieved. Finite strip solutions in combination with the semi-analytical sensitivity method deliver more accurate function and derivative values.
- The introduction of thickness as well as shape variation leads to a further improvement in the objective function of the optimal structures.

REFERENCES

1. B.I.Maisel, *Analysis of Concrete Box Beams Using Small-Computer Capacity*, C&CA, Development Report No. 5, 1982.London, United Kingdom.
2. A.C.Scordelis, "Folded plates for bridges", *Bull. Int. Assoc. Shell Spat Struct.*, Vol. 16 (1), No.57, 1974. Pp:29-38.
3. Y.K. Cheung, *Finite Strip Method in Structural Analysis*, Pergamon Press, Sydney, 1976.
4. A.G.Razaqpur and H.G.Li, "Thin walled multi-cell box girder finite element", *J. Structural Engineering*, Vol.117, No.10, 1991, pp.2953-2971.
5. A.G.Razaqpur and H.G.Li, "Refined analysis of curved thin-walled multi-cell box girders", *Computers and Structures*, Vol.53, No.1, 1994, pp.131-142.
6. D.J.Dawe and V.Peshkam, "Buckling and vibration of finite-length composite prismatic plate structures with diaphragm ends", *Comp. Meth. App. Mech. Engng.*, Vol.77, 1989 pp.1-30.
7. E.Hinton, M.Özakça. and N.V.R.Rao, "Free vibration analysis and shape optimization of variable thickness prismatic folded plates and curved shells- Part I: finite strip formulation", *J. Sound and Vibration*, Vol.181(4), 1995 pp.553-556.
8. E.Hinton and N.V.R Rao, "Analysis and shape optimization of variable thickness prismatic folded plates and curved shells. Part 1: finite strip formulation", *Thin Walled Structures*, Vol.17, 1993, pp.81-111
9. O.C.Zienkiewicz and J.S.Campbell, "Shape optimization and sequential linear programming", *Optimum Structural Design*. Eds. R.H. Gallagher and O.C. Zienkiewicz, Chapter 7, John Wiley, Chichester, 1973.
10. D.Hartman, and M.Neumann, "Structural optimization of a box girder bridge by means of the finite strip method", *Computer Aided Optimum Design of Structures*, Eds. Brebbia, C.A. and Hernandez, S., 1989 pp.337-346.
11. E.Hinton and N.V.R Rao, "Structural shape optimization of shells and folded plates using two noded finite strips", *Computers and Structures*, Vol.46, 1994, pp.1055-1071.
12. E.Hinton and N.V.R Rao, "Analysis and shape optimization of variable thickness prismatic folded plates and curved shells. Part II: shape optimization", *Thin Walled Structures*, Vol.17, 1993, pp.161-183.
13. I.D.Faux and M.JPratt, *Computational Geometry for Design and Manufacture*, 1979, Ellis Horwood, Chichester.

14. J.Sienz, *Integrated Structural Modeling Adaptive Analysis and Shape Optimization*, Ph.D. thesis, 1994, University College of Swansea.
15. N.V.RRao and E.Hinton, "Analysis and optimization of prismatic plate and shell structures with curved planform Part I: finite strip formulation", *Computers and Structures*, Vol.52, 1992, pp. 323-339.
16. K.Svanberg, "The method of moving asymptotes- a new method for structural optimization", *Int. J. Numerical Methods in Engineering*, Vol.23, 1987, pp.359-373.
17. R.G.Sisodiya and A.Ghali, "Analysis of box girder bridges of arbitrary shape", *IABSE Publication*, Vol.32, 1992, pp.203-217.
18. M.S.Cheung and Y.K.Cheung, "Analysis of curved box girder bridge by finite strip method", *IABSE Publication*, Vol. 31(1), 1971, pp.1-19.